

# Preparation of H-ZSM-5 Nano-Zeolite Using Mixed Template Method and its Activity Evaluation for Methanol to DME Reaction

S. Abbasian, M. Taghizadeh\*

Chemical Engineering Department, Babol University of Technology, Babol, I. R. Iran

(\*) Corresponding author: m\_taghizadehfr@yahoo.com

(Received: 04 April 2014 and accepted: 16 Aug. 2014)

## Abstract:

*H-ZSM-5 nano-zeolites were synthesized by hydrothermal method using tetrapropylammonium hydroxide (TPAOH) as a template in the presence of various TPABr concentrations. The effect of different TPABr/TPAOH molar ratios was studied on the catalytic performance of dehydration of methanol to dimethyl ether (DME) in a fixed bed reactor under the same operating conditions ( $T=300^{\circ}\text{C}$ ,  $P=1\text{ atm}$ , and  $\text{WHSV}=26\text{ h}^{-1}$ ). The prepared catalysts were characterized by XRD, SEM, BET and  $\text{NH}_3$ -TPD. The characterization results showed that the crystal sizes of the catalysts enlarge by increasing the concentration of TPABr in the synthesis reaction mixture. It was observed that H-form zeolite catalysts were active and selective for DME synthesis. These catalysts showed a high methanol conversion and also very high DME selectivity. It was found that by addition of up to 10 mole% TPABr in the synthesis reaction mixture, no significant effect was observed on the physical and chemical properties and catalytic activity of prepared catalysts.*

**Keywords:** Methanol dehydration, Dimethyl ether (DME), H-ZSM-5 nano-zeolite, Hydrothermal method, Mixed template.

## 1. INTRODUCTION

The importance of DME (dimethylether) as an alternative clean fuel for diesel has recently received growing attention due to some of its important properties like low CO and NO<sub>x</sub> emission and near zero smoke and other environmental friendly properties and high energy content [1–5].

Methanol is converted to DME by dehydration of methanol (Eq. 1) on acid catalysts [6]:



Many different solid acid catalysts such as  $\gamma$ -alumina,  $\gamma$ -alumina modified with silica and phosphorus, and zeolites (chabazites, mordenites,

SAPOs, H-ZSM-5, H-Y,...) in a temperature range of 250–400°C and pressures up to 18 bar have been used for DME synthesis [7–10].

In 1972 a kind of high-silica zeolite was found and reported by Argauer and Landolt from Mobil Oil Corporation which was called ZSM-5 [11]. This zeolite has received much attention due to its particular structure and physical-chemical performance, shape selectivity, stability and the flexibility, so it has been used in a variety of processes, such as dehydration of methanol, conversions of methanol to olefins (MTO) and gasoline (MTG), and FCC process [12–17]. Since 1972, extensive research has been carried out particularly to find catalysts having higher selectivity for the ether formation and less tendency to coke formation to

prevent catalyst deactivation and ultimately stop dehydration process. Accordingly, many researchers have tried to find a modified catalyst structure and/or formulation in order to optimize the DME production as well as improve the catalyst stability [18–22].

ZSM-5 is synthesized by a variety of organic templates, in which tetrapropylammonium cation (TPA<sup>+</sup>) is known as the most effective templating agent among them. Despite the excellent templating effect of TPA<sup>+</sup> cations they can create many problems like poison production, waste water contamination or air pollution due to thermal decomposition of organic templating agents. One of the most important problems with regard to ZSM-5 is its high production cost and the main reason of this cost is due to tetrapropylammonium hydroxide (TPAOH) as direct templating agent [23–27]. Therefore, lowering the TPAOH concentration in the synthesis reaction mixture without reducing the catalytic activity of prepared catalyst would reduce running costs and possibly reduce the capital costs of the process as well.

Zhu *et al.* employed a double template system, where the TPAOH template was governing crystallization of the MFI zeolite phase and polyvinyl butyral was used as a mesopore directing agent [28]. Xin *et al.* used a combination of TPABr and [3-(trimethoxysilyl)propyl] octadecyl-dimethylammonium chloride to synthesize iron-exchanged ZSM-5 powders containing mesoporous aggregates of smaller than 50 nm microporous ZSM-5 particles and tested the catalytic activity of the zeolite in selective hydroxylation of benzene to phenol [29].

MFI membranes are synthesized in the presence of organic templates such as tetrapropylammonium hydroxide (TPAOH). Since TPAOH is expensive, the preparation of MFI zeolite membranes without organic template or with cheap substitute template such as tetrapropylammonium bromide (TPABr) has been reported to reduce membrane cost and minimize the intercrystalline gaps for improving membrane selectivity [30–33].

In the present work, H-ZSM-5 nano-zeolites were prepared by a hydrothermal crystallization method with mixed templating agents. We tried to replace

tetrapropyl ammonium bromide (TPABr) with TPAOH in different molar ratios because of its lower price. The physicochemical properties of prepared catalysts were characterized by XRD, SEM, BET and NH<sub>3</sub>-TPD and their performance was evaluated in the catalytic dehydration of methanol to DME process using a fixed-bed flow reactor under the same operating conditions.

## 2. EXPERIMENTAL

### 2.1. Materials

The reactant materials used in this study were aluminum nitrate nonahydrate (ANN; Al(NO<sub>3</sub>)<sub>3</sub>•9H<sub>2</sub>O, 98.5 wt%, Merck) as aluminum source, tetrapropylammonium hydroxide solution (TPAOH, C<sub>12</sub>H<sub>29</sub>NO, 40% aqueous solution, Merck) and tetrapropylammonium bromide (TPABr, C<sub>12</sub>H<sub>28</sub>NBr, 99 wt%, Merck) as direct template agent, sodium hydroxide (NaOH, 98 wt%, Merck) and tetraethyl orthosilicate (TEOS, Si(OC<sub>2</sub>H<sub>5</sub>)<sub>4</sub>, 98 wt%, Merck) as a source of silica.

### 2.2. Catalyst preparation

The reaction mixture for the hydrothermal synthesis of Z-xBr (four batches) had the following molar compositions: 0.24Al<sub>2</sub>O<sub>3</sub>:60SiO<sub>2</sub>:(21.4-x) TPAOH:xTPABr:xNaOH:650H<sub>2</sub>O. First, the alumina source and 1/2 of required distilled water and TPAOH were mixed together in a polypropylene bottle with stirring at about 15 min until aluminum nitrate was completely dissolved. Then the rest of water and the required amounts of sodium hydroxide and TPABr were added to the solution and stirred briefly to dissolve the solid TPABr and NaOH.

Next, TEOS was added dropwise to the reaction mixture. The solution was stirred for 3 h at room temperature to hydrolyze TEOS completely. The resulting clear gel was then placed in a Teflon-lined stainless steel autoclave under static conditions at 180°C for 72 h. The white solid product was washed with distilled water several times until the pH reached about 7. The white solid product was centrifuged at a speed of 15000 rpm, washed several times with double distilled water, dried overnight at

105°C and calcinated in air at 550°C for 10 h at a heating rate of 3.5°C/min to remove residual water, ammonia, ammonium nitrate and the structure directing agent (TPA<sup>+</sup>). In the samples which NaOH was used, the Na-form zeolites were obtained. Na-ZSM-5 zeolites have been converted into the H-form by three consecutive ion-exchanges using an excess of 1 M aqueous NH<sub>4</sub>NO<sub>3</sub> with a solution/zeolite ratio of 10 ml/g at 80°C for 1 h and resulting samples were dried at 105°C and calcinated again at 520°C for 3 h.

The samples are designated as Z-xBr, in which x was varied from 0 to 3.21 resulted in a decrease in the amount of TPABr by 0 to 15 percent in the synthesis reaction mixture, respectively.

### 2.3. Characterization

The surface area (SBET), total pore volume (V<sub>p</sub>), and mean pore diameter (dp) of the calcined nanocrystalline ZSM-5 samples were measured by N<sub>2</sub> adsorption at -196°C using the Brunauer-Emmett-Teller (BET) method on a Belsorp mini II series instrument (BelJapan).

Powder X-ray diffraction patterns (EQuinox 3000, INEL, France, X-ray diffractometer using a Cu K $\alpha$  radiation source with  $\lambda = 1.5406 \text{ \AA}$  and nickel filter) were recorded with 2 $\theta$  range of 0–80 degrees with 1 s/step and 0.03 step size. The peaks between 2 $\theta = 21.5^\circ$  and 24° were calculated to obtain the relative crystallinity of the samples compared to the pattern (JCPDS No. 42–24).

The acidic properties of the samples were measured via temperature programmed desorption of ammonia (NH<sub>3</sub>-TPD), using a Pulse ChemiSorb 2705 instrument (Micrometrics, Norcross, GA) with a conventional flow device, which equipped with an online thermal conductivity detector (TCD). In a typical analysis, 0.3 g of the sample was degassed at 500°C under a helium flow rate of 50 ml/min at a heating rate of 10°C/min for 120 min. Next, the sample was saturated with pure NH<sub>3</sub> for 120 min when it was cooled to 100°C. The sample was then purged with a helium flow for 60 min to remove weakly and physically adsorbed ammonia on the surface of the catalyst. Afterwards, the sample was cooled to room temperature and then heated again

under a flow of helium carrier gas (50 ml/min) at a rate of 10°C/min, from 35 to 800°C. Finally, the amount of NH<sub>3</sub> in the effluent was measured using TCD and recorded as a function of the temperature. Scanning electron microscopy was performed on the samples to determine their particle size and morphology using a TESCAN-VEGA SEM instrument.

### 2.4. Catalytic tests

The dehydration of methanol was performed in a fixed-bed reactor at atmospheric pressure. A fixed-bed stainless steel reactor having 10 mm of inner diameter and 920 mm length was used. In each test, 0.9 g of the catalyst was packed between quartz wool plugs and placed in the middle part of the reactor. Pure methanol was pumped from a feed tank by the stroking pump (LMI Milton Roy series P-133) at a flow rate and weight hourly space velocity (WHSV) of 0.5 ml/min and 26 h<sup>-1</sup>, respectively. The reactor effluent was analyzed quantitatively by an online GC (Teif Gostarfaraz Co., Iran) equipped with HayeSep Q column and flame ionization detector, applying temperature programming starting at 35°C (2 min at the initial temperature) and heating to 160°C (4 min at the final temperature) at a rate of 10°C min<sup>-1</sup>. The reaction performance results, including methanol conversion, DME selectivity and yield, were subsequently calculated.

## 3. RESULTS AND DISCUSSION

### 3.1. Characterization results

Figure 1 shows XRD patterns of samples crystallized using different molar ratios of templates. The XRD patterns show peaks in the 2 $\theta$  range of 21.5°–24°, which correspond to specific peaks of the H-ZSM-5 sample (JCPDS No. 42–24), and no peaks corresponding to Na-containing phases are detected. It is seen that all the samples are highly crystalline. The average crystal size of synthesized samples is summarized in Table 1 which was estimated using Scherer equation.

The N<sub>2</sub> adsorption-desorption isotherms of the samples are shown in Figure 2. As it is evident, all

the samples can be classified as a type I isotherm and they indicate the presence of low fractions of mesopores structure to some extent.

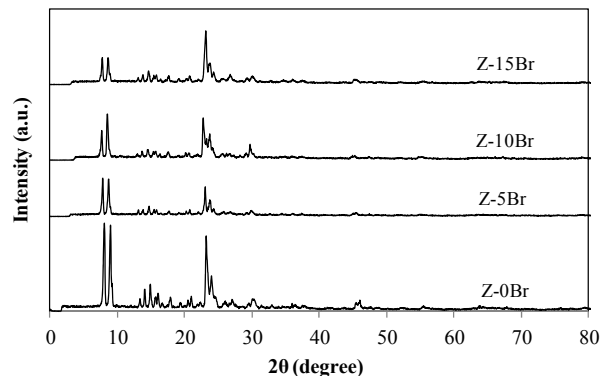


**Figure 1:** XRD patterns of different calcined zeolites.

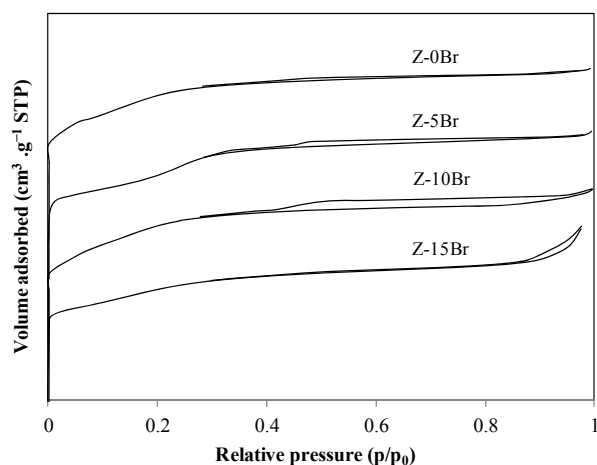


**Figure 2:**  $N_2$  adsorption-desorption isotherms of different zeolite samples.

The BET surface area, pore volume and pore diameter of the prepared catalysts are summarized

in Table 2. As seen, the BET surface area of Z-xBr samples decreased with increasing the amount of TPABr in zeolites, while the pore volume and pore diameter of the samples increased.

In order to understand the distribution of the surface acidity and the strength of the acid sites, a systematic study of  $NH_3$ -TPD measurements was performed. The  $NH_3$ -TPD profiles of H-ZSM-5 samples are shown in Figure 3. The results of ammonia TPD-titration that contain the amount of desorbed ammonia and acidity content of the prepared catalysts are summarized in Table 3. As shown in Figure 3, There are three desorption peaks in TPD profiles of catalysts with maxima in the range of 70–240, 240–430 and 430–800°C, which can be ascribed to the  $NH_3$  desorbed from acid sites with low, medium and high strengths, respectively. The results showed that the total acidity of the catalysts decreased with increases in the TPABr molar ratio. Many researchers have reported that strong acid sites are responsible for the formation of hydrocarbons and acid sites of weak or intermediate strength are responsible for the selective formation of DME [22, 27]. Among the prepared catalysts, Z-0Br had the highest number of weak acid sites, followed by Z-5Br and Z-10Br. Therefore, it was expected that the Z-0Br has the highest methanol conversion and DME selectivity; but Z-5Br and Z-10Br have similar performance to Z-0Br.

Figure 4 shows the SEM micrographs of the Z-xBr samples synthesized in different concentrations of TPABr after calcinations. Our SEM study revealed that the particles present in the prepared samples have a uniform distribution and their morphologies are regular. The average particle sizes estimated from the SEM images

**Table 1:** Crystal size and molarity of catalysts

Catalyst	pH*	Si/Al	TPAOH/SiO <sub>2</sub>	TPABr/SiO <sub>2</sub>	OH <sup>-</sup> /SiO <sub>2</sub>	H <sub>2</sub> O/SiO <sub>2</sub>	Crystal size (nm)
Z-0Br	11.59	125	0.36	0	0.35	10.8	26.64
Z-5Br	11.48	125	0.34	0.018	0.35	10.8	65.09
Z-10Br	11.47	125	0.32	0.036	0.35	10.8	75.68
Z-15Br	11.41	125	0.30	0.053	0.35	10.8	80.55

\* pH values were measured before crystallization

**Table 2:**Physical properties of samples

Catalyst	Surface area (m <sup>2</sup> /g)	Pore volume x 10 <sup>3</sup> (ml/g)	Pore diameter (nm)
Z-0Br	428.78	403.8	1.90
Z-5Br	420.81	406.8	1.97
Z-10Br	418.27	422.7	2.03
Z-15Br	415.44	421.3	2.18

**Table 3:**Results of NH<sub>3</sub>-TPD analysis of different H-ZSM-5 catalysts

Catalyst	Maximum desorption temperature (°C)	Amount of NH <sub>3</sub> (mmol/g <sub>cat</sub> )	Total acidity (mmol/g <sub>dry sample</sub> )
Z-0Br	74	0.294	0.66
	343	0.032	
	711	0.334	
Z-5Br	72	0.281	0.61
	300	0.015	
	725	0.318	
Z-10Br	70	0.277	0.46
	–	–	
	700	0.178	
Z-15Br	71	0.08	0.2
	322	0.027	
	735	0.093	

increased with increasing TPABr concentration in the synthesis reaction mixture. These results are in good agreement with the XRD results.

### 3.2. Catalytic performance in the dehydration of methanol

In order to find the difference in the performance of the prepared catalysts in terms of methanol conversion and DME selectivity, all catalyst samples were evaluated for catalytic dehydration of methanol to dimethyl ether under the same and steady-state operating conditions

(300°C, 1 atm and WHSV of 26 h<sup>-1</sup>) for 3 h in a fixed bed reactor (ID=10 mm, L=920 mm). According to our previous research, the conversion reaches 90% at a temperature of 300°C and WHSV of 26 h<sup>-1</sup>. To evaluate the reaction for a condition near the equilibrium, these temperature and WHSV values have been selected [13, 22]. The changes in the yield of DME, methanol conversion and DME selectivity of various catalysts are listed in Table 4.

Methanol conversion, selectivity and yield of DME were defined as follows:

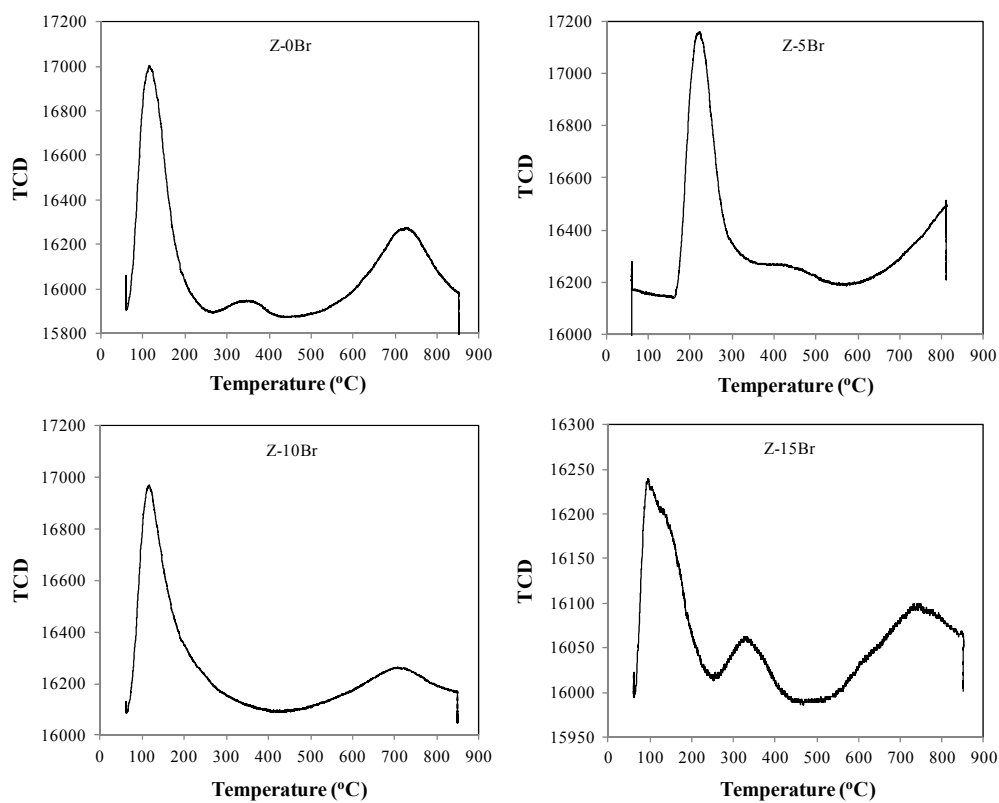


**Figure 3:**  $NH_3$ -TPD profiles of synthesized catalysts.

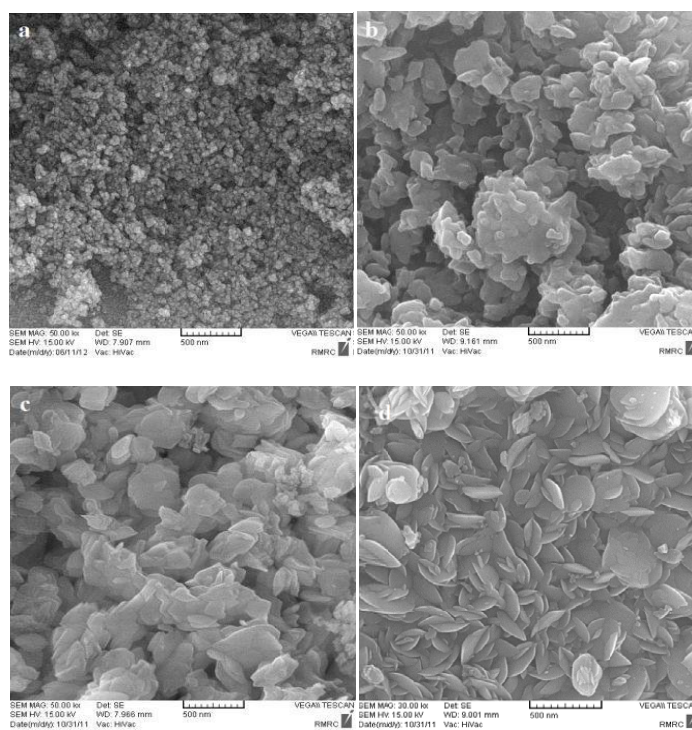


**Figure 4:** SEM images of samples: a) Z-0Br, b) Z-5Br, c) Z-10Br, d) Z-15Br.

$$\text{MeOH conversion} = \frac{\text{MeOH moles (initial amount)} - \text{MeOH moles (final amount)}}{\text{MeOH moles (initial amount)}} \times 100 \quad (2)$$

$$\text{DME selectivity} = \frac{\text{DME moles produced} \times 2}{\text{MeOH moles (initial amount)} - \text{MeOH moles (final amount)}} \times 100 \quad (3)$$

$$\text{Yield of DME} = (\text{MeOH conversion}) \times (\text{DME selectivity}) \quad (4)$$

The results in Table 4 show that all the catalysts exhibit a very high conversion of methanol. As to the selectivity, no considerable differences were found among the samples during catalyst testing, though the DME selectivity over Z-0Br and Z-5Br was slightly higher than others. The maximum yield to DME was about 90% on Z-0Br, although the results showed that the Z-5Br and Z-10Br had a very good and comparable performance with Z-0Br. These differences are related to their surface area and weak or intermediate number of acidic sites responsible for the selective formation of DME (Tables 2 and 3).

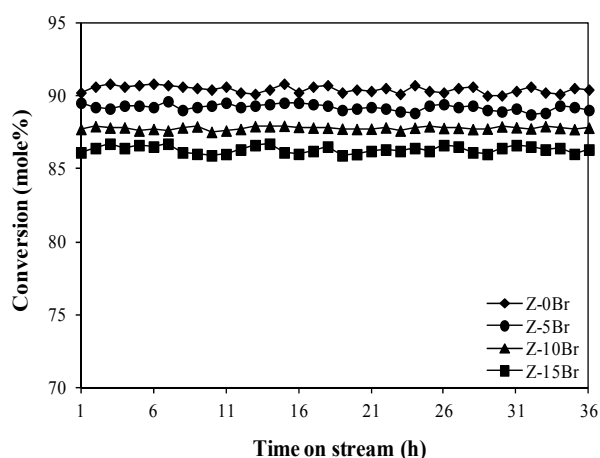


**Figure 5:** Variation of methanol conversion of different samples as a function of time on stream at  $T = 300^\circ\text{C}$ ,  $P = 1 \text{ atm}$ , and  $\text{WHSV} = 26 \text{ h}^{-1}$ .

The long-term stability of the prepared catalysts after 36 h of reaction is shown in Figure 5. As it can be seen, all samples are stable and showed excellent stability for the dehydration reaction.

To determine the main product and byproduct, a gaseous calibration mixture including  $\text{CH}_4$  and  $\text{C}_2\text{-C}_4$  olefin/paraffin components was used, which was probably manufactured as the byproduct of methanol dehydration reaction. In this work,  $\text{C}_2\text{H}_4$  and  $\text{C}_3\text{H}_6$  were the main byproducts which were slightly produced in DME synthesis because of low temperature. Figure 6 shows quantity of the main byproducts over different catalysts.

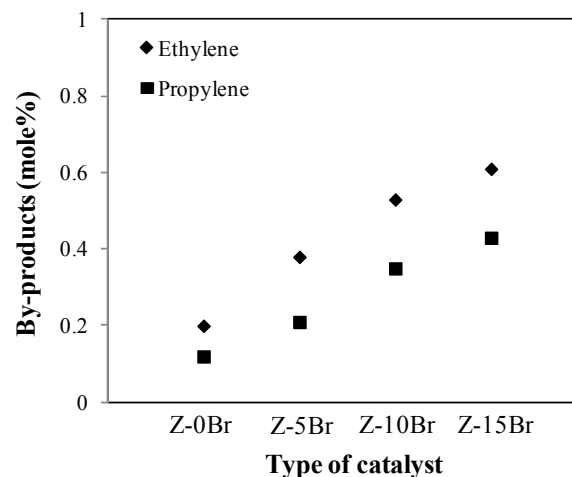


**Figure 6:** Variation of the main byproduct concentration of different H-ZSM-5 catalysts.

**Table 4:** Catalytic activities of different H-ZSM-5 catalysts

Catalyst	MeOH conversion (%)	DME selectivity (%)	DME yield (%)
Z-0Br	90.92	99.68	90.63
Z-5Br	89.5	99.41	88.97
Z-10Br	87.98	99.12	87.21
Z-15Br	86.7	98.96	85.80

## 4. CONCLUSION

A mixture of two templates of TPAOH and TPABr was used in the synthesis of ZSM-5 nano-zeolite due to the high cost of using templates, especially TPAOH. The effects of TPABr/TPAOH molar ratios on zeolite crystallization in the synthesis reaction mixture with a molar composition of  $0.24\text{Al}_2\text{O}_3:60\text{SiO}_2:(21.4-x)\text{TPAOH}:x\text{TPABr}:x\text{NaOH}:650\text{H}_2\text{O}$  were investigated and H-ZSM-5 nano-zeolites were successfully synthesized by the hydrothermal crystallization method. All prepared H-form zeolites were active and selective for methanol dehydration to DME.

The structure and morphology of the catalysts were studied by X-ray diffraction (XRD) and BET. XRD patterns showed that the extent and percentage of crystallinity of catalysts did not differ significantly and all the catalysts were in nanoscale range. Also, with increasing TPABr concentration in the synthesis reaction mixture, crystal sizes increased. BET results showed that by increasing the amount of TPABr or TPABr/TPAOH molar ratio in the synthesis reaction mixture, pore volume and average pore diameters of the catalysts increased but the surface area decreased.

The  $\text{NH}_3$ -TPD analysis demonstrated that the sample with smaller crystallite size possessed higher concentration of weak and medium acidic sites and consequently a higher catalytic activity. The experimental data indicated that all the catalysts show very high conversion with nearly complete selectivity in methanol dehydration to DME. The addition of up to 10 mole% TPABr to TPAOH in the synthesis reaction mixture does not significantly affect the properties and performance of prepared catalysts; an economic saving in preparation cost can be achieved.

## ACKNOWLEDGMENT

This work was financially supported by Iranian Nanotechnology Initiative Council.

## REFERENCES

1. S. Sidhu, J. Graham, R. Striebich: *Chemosphere*, Vol. 42, (2001), pp. 681–690.
2. T. A. Semelsberger, R. L. Borup, H. L. Greene: *J. Power Sources*, Vol. 156, (2006), pp. 496–511.
3. G. A. Olah, A. Goepfert, G. K. S. Prakash: *J. Org. Chem.*, Vol. 74, (2009), pp. 487–498.
4. Y. Adachi, M. Komoto, I. Watanabe, Y. Ohno, K. Fujimoto: *Fuel*, Vol. 79, (2000), pp. 229–234.
5. Z. Gao, W. Huang, L. Yin, K. Xie: *Fuel Process. Technol.*, Vol. 90, (2009), pp. 1442–1446.
6. G. Moradi, J. Ahmadpour, F. Yaripour: *Energy Fuels*, Vol. 22, (2008), pp. 3587–3593.
7. X. D. Peng, G. E. Parris, B. A. Toseland, P. J. Battavio: US Patent, No. 5, 753, 716, (1998).
8. J. H. Kim, M. J. Park, S. J. Kim, O. S. Joo, K. D. Jung: *Appl. Catal. A: Gen.*, Vol. 264, (2004), pp. 37–41.
9. T. Shikada, K. Fujimoto, Y. Ohno, T. Ogawa, M. Mizuguchi, M. Ono: US Patent No. 5,446,720 (2006).
10. B. Wang, Y. Wen, W. Huang: *Energy Sources, Part A*, Vol. 35, (2013), pp. 1590–1596.
11. R. J. Argauer, G. R. Landolt: US Patent, No. 3,702,886 (1972).
12. Y. Cheng, L. J. Wang, J. S. Li, Y. C. Yang, X. Y. Sun: *Mater. Lett.*, Vol. 59, (2005), pp. 3427–3430.
13. S. Hosseini, M. Taghizadeh, A. Eliassi: *J. Nat. Gas Chem.*, Vol. 21, (2012), pp. 344–351.
14. M. Firoozi, M. Baghalha, M. Asadi: *Catal. Commun.*, Vol. 10, (2009), pp. 1582–1585.
15. J. Liu, C. X. Zhang, Z. H. Shen, W. M. Hua, Y. Tang, W. Shen, Y. H. Yue, H. L. Xu: *Catal. Commun.*, Vol. 10, (2009), pp. 1506–1509.
16. S. N. Khadzhiev, N. V. Kolesnichenko, N. N. Ezhova: *Pet. Chem.*, Vol. 48, (2008), pp. 325–334.
17. R. V. Ermakov, V. A. Plakhotnik: *Pet. Chem.*, Vol. 48, (2008), pp. 1–5.
18. M. Xu, J. H. Lunsford, D. W. Goodman, A. Bhattacharyya: *Appl. Catal. A: Gen.*, Vol. 149, (1997), pp. 289–301.

19. J. Fei, Z. Hou, B. Zhu, H. Lou, X. Zheng: Appl. Catal. A: Gen., Vol. 304, (2006), pp. 49–54.
20. S. D. Kim, S. C. Baek, Y. J. Lee, K. W. Jun, M. J. Kim, I. S. Yoo: Appl. Catal. A: Gen., Vol. 309, (2006), pp. 139–143.
21. F. Raoof, M. Taghizadeh, A. Eliassi, F. Yaripour: Fuel, Vol. 87, (2008), pp. 2967–2971.
22. S. Hassanpour, F. Yaripour, M. Taghizadeh: Fuel Process. Technol., Vol. 91, (2010), pp. 1212–1221.
23. J. C. Védrine, A. Auroux, P. Dejaifve, V. Ducarme, H. Hoser, S. Zhou: J. Catal., Vol. 73, (1982), pp. 147–160.
24. N. Y. Chen, W. E. Garwood: J. Catal., Vol. 52, (1978), pp. 453–458.
25. V. Valtchev, S. Mintova: Microporous Mesoporous Mater., Vol. 43, (2001), pp. 41–49.
26. Y. Wang, Y. Tang, A. Dong, X. Wang, N. Ren, Z. Gao: J. Mater. Chem., Vol. 12, (2002), pp. 1812–1818.
27. V. Siva Kumar, A. H. Padmasri, C. V. V. Satyanarayana, I. Ajit Kumar Reddy, B. David Raju, K. S. Rama Rao: Catal. Commun., Vol. 7, (2006), pp. 745–751.
28. H. Zhu, Z. Liu, D. Kong, Y. Wang, X. Yuan, Z. Xie: J. Colloid Interface Sci., Vol. 331, (2009), pp. 432–438.
29. H. Xin, A. Koekkoek, Q. Yang, R. van Santen, C. Li, E.J.M. Hensen: Chem. Commun., Vol. 48, (2009), pp. 7590–7592.
30. F. Meng, Y. Wang, L. Wang, R. Yang, T. Zhang: J. Mol. Catal. A: Chem., Vol. 335, (2011), pp. 105–111.
31. P. Chen, X. S. Chen, K. Tanaka, H. Kita: Chem. Lett., Vol. 36, (2007), pp. 1078–1079.
32. P. Chen, X. B. Chen, X. S. Chen, H. Kita: J. Membr. Sci., Vol. 330, (2009), pp. 369–378.
33. R. F. Zhou, M. H. Zhu, X. S. Chen, H. Kita: Chem. Lett., Vol. 39, (2010), pp. 388–389.

